Electronic Supplementary Material (ESI) for: Unconventional co-existence of plasmon and thermoelectric activity in In:ZnO nanowires

Alessandra Catellani

Istituto Nanoscienze CNR-NANO-S3, I-41125 Modena, Italy and

CNR-IMEM, Parco Area delle Scienze, 37A, I-43100 Parma, Italy

Alice Ruini

Istituto Nanoscienze CNR-NANO-S3, I-41125 Modena, Italy and

Dipartimento di Fisica, Informatica e Matematica,

Universitá di Modena e Reggio Emilia, I-41125 Modena, Italy

Marco Buongiorno Nardelli

Department of Physics, University of North Texas, Denton, TX 76203, USA and

Center for Materials Genomics, Duke University, Durham, NC 27708, USA

Arrigo Calzolari*

Istituto Nanoscienze CNR-NANO-S3, I-41125 Modena, Italy and

Department of Physics, University of North Texas, Denton, TX 76203, USA

PACS numbers: 73.22.Lp,72.20.Pa,71.45.Gm,79.10.-n,63.22.Gh,71.15.Mb,81.05.Dz

*Electronic address: arrigo.calzolari@nano.cnr.it

S1: Single particle orbitals and density of states

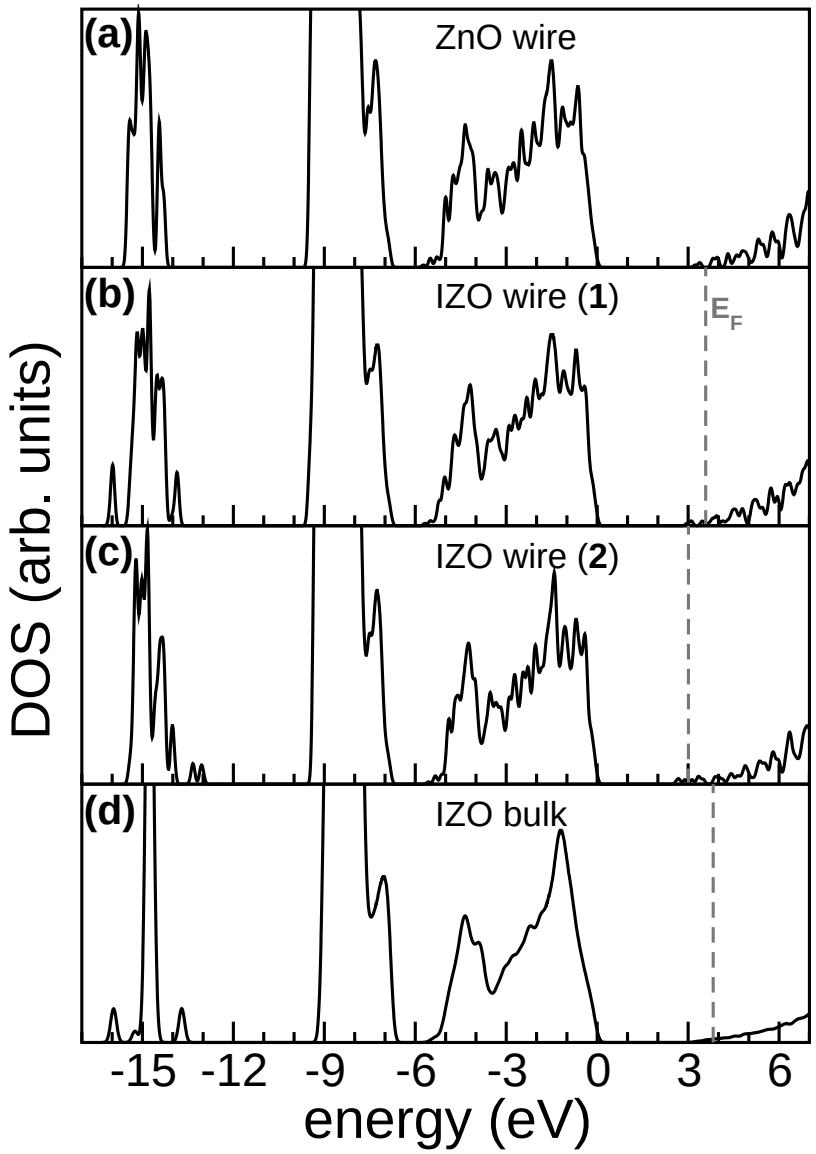

FIG. S1: DOS of (a) un-doped ZnO wire, (b) IZO wire, configuration **1**, (c) IZO wire, configuration **2**, (d) IZO bulk, for the entire calculated energy range. Dashed vertical lines identify the Fermi level of each metallic system. Zero energy reference is set to the valence band top of un-doped hosts.

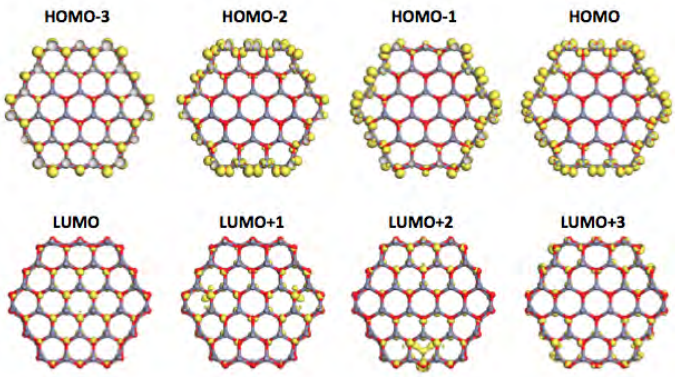

FIG. S2: Isosurface plots of selected Kohn Sham single particle orbitals at Γ point for undoped ZnO wire.

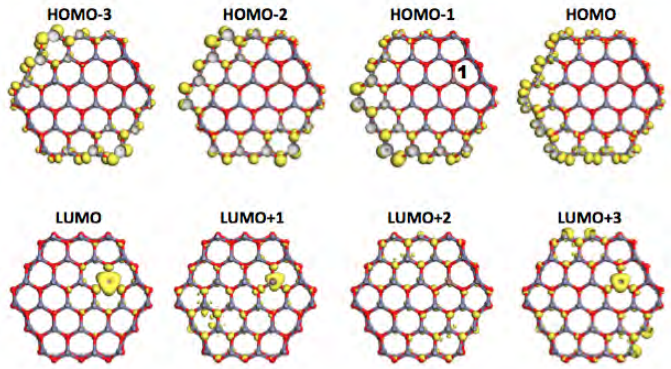

FIG. S3: Isosurface plots of selected Kohn Sham single particle orbitals at Γ point for IZO(**1**) wire.

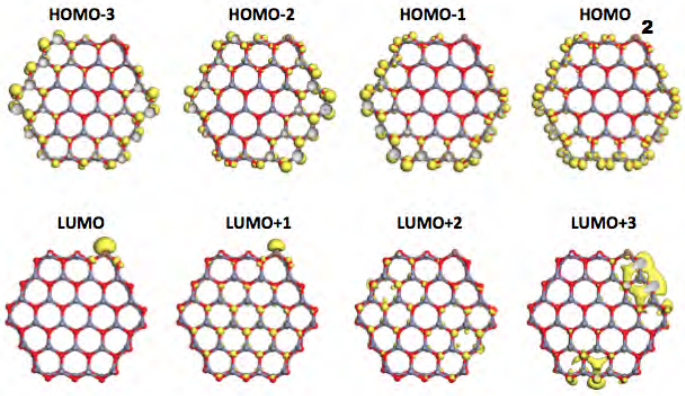

FIG. S4: Isosurface plots of selected Kohn Sham single particle orbitals at Γ point for IZO(**2**) wire.

S2: Complex dielectric function analysis

For the analysis of the optical properties of the systems presented in the main text we adopted a solid-state implementation of a Drude-Lorentz expression for the complex dielectric function $\hat{\epsilon}(\omega) = \epsilon_1 + i\epsilon_2$. [1] The real ($\epsilon_1$) and imaginary ($\epsilon_2$) part of the dielectric function are respectively:

$$\epsilon_1(\omega) = 1 - \omega_p^2 \sum_{\mathbf{k},n} f_{\mathbf{k}}^{n,n} \frac{1}{\omega^2 + \eta^2} + \omega_p^2 \sum_{\mathbf{k},n\neq n'} f_{\mathbf{k}}^{n,n'} \frac{\omega_{\mathbf{k},n,n'}^2 - \omega^2}{(\omega_{\mathbf{k},n,n'}^2 - \omega^2)^2 + (\Gamma\omega)^2}, \tag{1}$$

and

$$\epsilon_2(\omega) = \omega_p^2 \sum_{\mathbf{k},n} f_{\mathbf{k}}^{n,n} \frac{\eta}{\omega(\omega^2 + \eta^2)} + \omega_p^2 \sum_{\mathbf{k},n\neq n'} f_{\mathbf{k}}^{n,n'} \frac{\Gamma\omega}{(\omega_{\mathbf{k},n,n'}^2 - \omega^2)^2 + (\Gamma\omega)^2}, \tag{2}$$

where ω_p is the plasma frequency, $\hbar\omega_{\mathbf{k},n,n'} = E_{\mathbf{k},n} - E_{\mathbf{k},n'}$ is the vertical band-to-band transition energy between occupied and empty Bloch states labeled by the quantum numbers $\{\mathbf{k}, n\}$ and $\{\mathbf{k}, n'\}$. $\eta, \Gamma \to 0^+$ are the Drude-like and Lorentz-like relaxation terms associated to intra-band and inter-band transitions respectively, while $f_{\mathbf{k}}^{n,n}$ and $f_{\mathbf{k}}^{n,n'}$ are the corresponding oscillator strengths. See also Ref. [2] for further details.

The results of the dielectric function simulations are shown in Figure S5. The results are in agreement with what observed for Al-ZnO systems: The undoped wire exhibits the typical features of a semiconductor: ϵ_1 is always positive and reaches the dielectric constant value $\epsilon^\infty = 1.3$ in the limit for $\omega \to 0^+$, although this value is rather smaller than the 3D ZnO case ($\epsilon^\infty = 3.0$). The imaginary part ϵ_2, which is proportional to the absorption spectrum, is zero in the IR and visible range and has the first adsorption edge in the UV (i.e. the ZnO wire is transparent).

After the inclusion of the In impurities, the dielectric function assumes a metallic behavior: in the low-energy range ϵ_2 is positive and diverges for $\omega \to 0^+$, which corresponds to the *dc* conductivity of simple metals, while ϵ_1 is negative, in agreement with the formation of a free electron gas. In the UV range, the energy position of the lowest-energy peak, E_g^{opt}, corresponds to the interband valence-to-conduction absorption edge, and is system-dependent (see Table 1 main text). A doping-induced blue-shift of the absorption edge is present in all cases, and may be explained in terms of the Burnstein-Moss model. The transparency in the visible range along with the electrical n-type characteristics confirms the TCO behavior displayed by both wire and bulk IZO compounds.

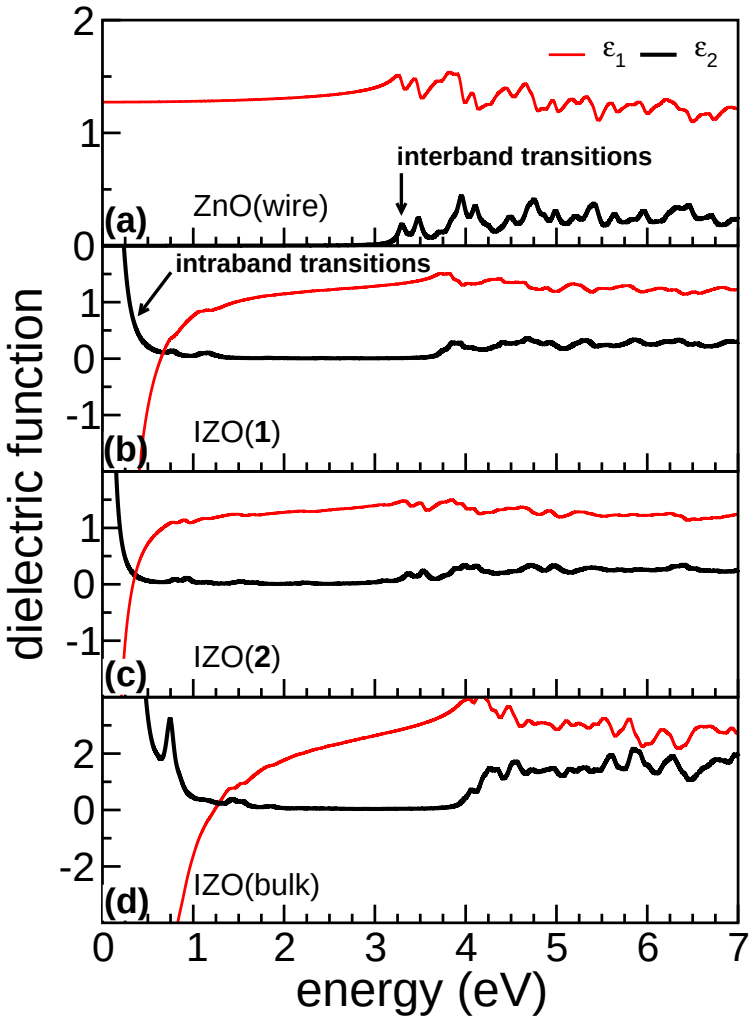

FIG. S5: Real (red line) and imaginary (black line) part of complex dielectric function $\hat{\epsilon}$ of (a) undoped ZnO wire, (b) IZO wire, configuration **1**, (c) IZO wire, configuration **2**, (d) IZO bulk.

S3: Thermal transport analysis

In aperiodic system, at a given wavenumber, the quantum transmittance $\mathcal{T}_{ph}$ is a proportional to the number of transmitting channels available for phonon mobility, which are equal to the number of conducting bands at the same energy. This is proved in Figure S6, where the phonon band structucture and the transmittance plot are compared.

The phonon thermal conductance K_{ph} can be obtained from $\mathcal{T}_{ph}$ via direct integration:

$$K_{ph}(T) = \frac{1}{2\pi\hbar}\int_0^\infty d(\hbar\omega)\mathcal{T}_{ph}(\omega)\hbar\omega\left[\frac{\partial n(T,\omega)}{\partial T}\right], \tag{3}$$

where $n(T,\omega)$ is the Boltzman distribution at temperature T. Resulting conductance plot is displayed in Figure S7.

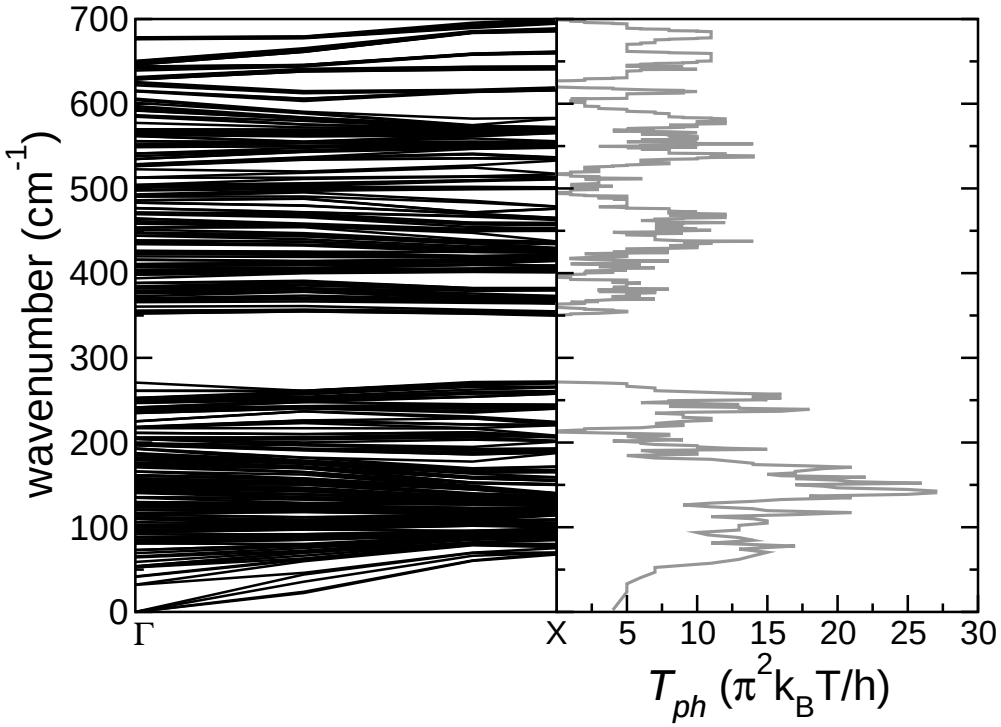

FIG. S6: (left) Phonon dispersion relation along the direction parallel to the wire axis. (right) Thermal transmittance spectrum.

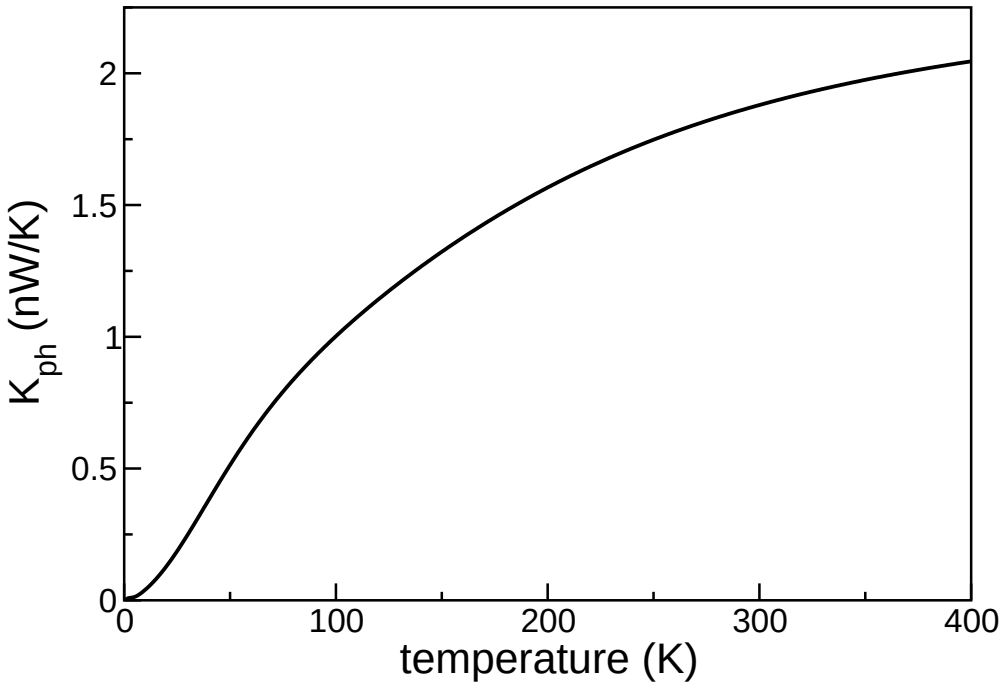

FIG. S7: Phonon thermal conductance of undoped ZnO wire, as a function of temperature.

S4: Figure of merit in coherent approximation

The figure of merit of a thermoelectric material is defined as:

$$ZT = S^2 \sigma_{el} T / \kappa_t, \tag{4}$$

where S is the Seebeck coefficient, σ_{el} is the electrical conductivity, T is the absolute temperature, and $\kappa_t = \kappa_{el} + \kappa_{ph}$ is the thermal conductivity, which includes contributes from both electrons (κ_{el}) and phonons (κ_{ph}), respectively. In the coherent transport approximation, i.e. in the absence of inelastic scattering processes, the figure of merit reduces to:

$$ZT = S^2 G_{el} T / K_t, \tag{5}$$

where G_{el} and $K_t = K_{el} + K_{ph}$ are the corresponding quantum conductance. The electron quantum conductance G_{el}, the electron contribution to thermal conductance K_{el} and the Seebeck coefficient S can be derived from the electronic transmission $\mathcal{T}_{el}$ by defining an intermediate function $L_n(\mu, T)$, of the chemical potential (μ) and the temperature: [3]

$$L_n(\mu, T) = \frac{2}{h} \int dE \mathcal{T}_{el} (E - \mu)^n \Big[= \frac{\partial f(E, \mu, T)}{\partial e} \Big] \tag{6}$$

By using the standard kinetic relations we obtain:

$$G_{el} = \frac{2e^2}{h} \mathcal{T}_{el}(\mu), \tag{7}$$

$$K_{el}(\mu, T) = \frac{1}{T} \Big[L_2(\mu, T) - \frac{L_1(\mu, T)^2}{L_0(\mu, T)} \Big], \tag{8}$$

$$S(\mu, T) = \frac{1}{qT} \Big[\frac{L_1(\mu, T)}{L_0(\mu, T)} \Big] \tag{9}$$

that enter in the ZT expression.

[1] Colle, R.; Parruccini, P.; Benassi, A.; Cavazzoni, C. Optical properties of emeraldine salt polymers from ab initio calculations: comparison with recent experimental data. *J. Phys. Chem. B* **2007**, *111*, 2800–2805.

[2] Calzolari, A.; Ruini, A.; Catellani, A. Transparent Conductive Oxides as Near-IR Plasmonic Materials: The Case of Al-Doped ZnO Derivatives. *ACS Photonics* **2014**, *1*, 703–709.

[3] Grosso, G.; Pastori Parravicini, G. *Solid State Physics, 2nd Ed.*; Academic Press Elsevier Ltd., Amsterdam NL, 2014.